Reliability of ITER Diagnostic Pressure Gauges: Experimental Validation of Thermo-Mechanical Simulations

Alexey Arkhipov[a], Felix Mackel[a], Günter Haas[a], Jürgen Koll[a], Andrea Scarabosio[a], Hans Meister[a], Fabien Seyvet[b], Santiago Terron[b] and Philip Andrew[c]

[a]*Max-Planck Institute for Plasma Physics, Boltzmannstraße 2, D-85748 Garching, Germany*
[b]*Fusion for Energy, C/Josep Pla, n° 2, Torres Diagonal Litoral, Edificio B3, 08019 Barcelona, Spain*
[c]*ITER Organization, Route de Vinon-sur-Verdon, CS 90 046, 13067 St. Paul Lez Durance Cedex, France*

Diagnostic Pressure Gauges (DPG) shall provide measurements of the neutral gas pressure in ITER in 4 lower ports, 4 divertor cassettes and 2 equatorial ports. The DPG is a hot cathode ionization gauge where the filament (hot cathode) is heated up by a high electric current in order to reach a temperature sufficient for emission of electrons. The DPG will operate in an environment with strong magnetic field (up to 8 T). Hence, under mentioned operational conditions the filament of the gauge will be under high thermal stress and the influence of $\vec{j}\times\vec{B}$ forces. Finite element analyses (FEA) of the DPG sensor have been executed with the aim to determine the temperature distribution and to assess stress level and structural integrity of the filament and other gauge components. In cases where boundary conditions and material constants were not exactly defined, assumptions have been made accordingly. This, however, reduces the reliability of simulation results. In order to gain benchmarking data for validation of the performed simulations, experimental investigation of the filament temperature profile has been executed. Reliability tests are envisaged to investigate the operational margin of the gauge by identifying the minimum heating current required to produce sufficient emission current over a long period of time and the maximum current in a high magnetic field causing structural damage to the filament. Results of these tests allow measuring the accurateness of FEA, which delivers predictions of stability thresholds with respect to the heating current and magnetic field. Comparison of experimental data with results of FEA simulations are discussed in this paper.

Keywords: ITER, plasma diagnostics, pressure gauge, tungsten filament, FEA, testing.

1. Introduction

The design of the ITER diagnostic pressure gauges (DPG) is based on the design of the ASDEX pressure gauges (APG) [1], which are widely used for pressure measurements in present-day tokamaks and stellarators such as ASDEX Upgrade, DIIID, JET and W7-X [2]. The model of the gauge is shown in Fig. 1.

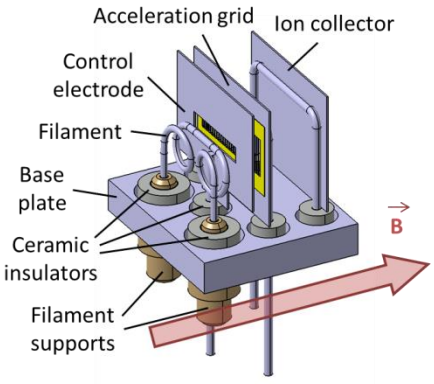

Fig. 1: Model of the APG sensor.

The diagnostic provides measurement of neutral gas density relying on the ionization of neutral gas by electrons emitted from the surface of the filament (hot cathode) and accelerated in a static electric field. In order to increase residence time of electrons and enhance sensitivity of the gauge electrodes are arranged along the axis parallel to force lines of acting magnetic field [1].

This on the other hand causes strong $\vec{j}\times\vec{B}$ forces on the filament, since heating current flows in perpendicular direction to the magnetic field. In contrast with the APGs operating at typical magnetic fields of 2-3.5 T the pressure gauges in ITER shall provide measurements at B-fields of up to 8 T meaning 3-4 times higher acting $\vec{j}\times\vec{B}$ forces [3]. In addition, the filament operates at high temperature. A consequence of these high temperatures is the decrease of the material elastic yield strength to the lower values. The superposition of the electromagnetic forces and thermal stresses with concurrent reduction of the material elastic yield strength might cause the failure of the filament. In case the stresses exceed the yield strength of the material it deforms resulting in possible failure of the whole diagnostic. For instance, deformed filament can touch control electrode forming a short circuit. Thus, the filament of the gauge is the most critical part within the unit that primarily limits lifetime of the DPG head.

The choice of the filament material is a crucial factor for its resistance. It has to be a refractory material with the ability to retain certain yield strength at high temperatures. The temperature required to emit electrons should be as low as possible. This translates into a low work function of the material. Often, a small amount of material, featuring a low work function, is added to a refractory material or it is applied to the surface. A suitable candidate is tungsten, which has the highest melting point of all elements. Addition of a small

author's email: alexey.arkhipov@ipp.mpg.de

amount (1 %-2 %) of ThO_2 or La_2O_3 reduces the work function considerably. As a consequence the material emits a sufficient electron current (~400 µA) at rather low temperatures of about 1800 K.

Within the test campaign, which is currently ongoing under a Framework Partnership Agreement with Fusion for Energy (FPA-364), it is planned to show reliability compliance among a number of preselected filament materials. The operational margin is assessed by identifying the minimum current required to produce sufficient emission current over a long period of time (3 months) and the maximum current in a high magnetic field (up to 8 T) causing structural damage to the filament. Testing strategy aims at finding a suitable and not the perfect solution. To this end, the tests will be interrupted after having found a satisfactory filament material.

Geometry of the filaments, which are currently used in test campaign, has been defined under a parametric FE analysis, which was executed within the ANSYS/APDL environment by the engineering company SRS Engineering Design under the F4E contract OMF-0457-01-10. During optimization process the temperature profiles along the filament and a stress level were calculated for several proposed shapes: “single spiral”, “multi spiral”, “circle”, “arc” and “mickey mouse”. For each shape the effects of a geometric variation, including the filament diameter, have been analyzed. According to performed parametric study, the filament with the diameter of 0.8 mm and conventional for APGs shape i.e. “single spiral” [1] has been confirmed as optimal one in terms of mechanical stability.

The same parametric model was used to simulate the experiment described in the Section 2. Analysis was done for the optimized filament. Detailed description of a parametric model and analysis approach is given in the Section 3. Comparison of obtained experimental data with simulation results is presented in the Section 4.

2. Measurement of the temperature profile of the filament

Knowledge of the filament temperature is essential for the further structural integrity analysis and for the estimation of the heating of the whole gauge head. By simultaneous measurements of the electron emission, it is possible to acquire the emission properties of the filament material. Recently, measurements of the temperature profile of the filament sample made of tungsten doped with 2 % of ThO_2 (WT 20) has been performed for several values of the heating current. This profile allows an estimation of the decrease of Young’s modulus and the yield stress of the material with increasing temperature. The aim of this test is to validate results of performed FE analysis and to “calibrate” the material properties, which are used for the calculations.

Testing has been performed at the IPP laboratory in a vacuum chamber with a base pressure of $<10^{-5}$ Pa equipped with two turbo pumps, cryo pump, feedback controlled gas feeding system, residual gas analyzer and combined Bayard-Alpert and Pirani gauge. Specific DPG head prototype (see Fig. 2) comprised of the base plate, the filament support that allows for exchange of the filament sample and the electron collector, accommodated above the filament, has been tested. Prototype was mounted on customized holder connected with the flange and inserted in vacuum vessel (see Fig. 2).

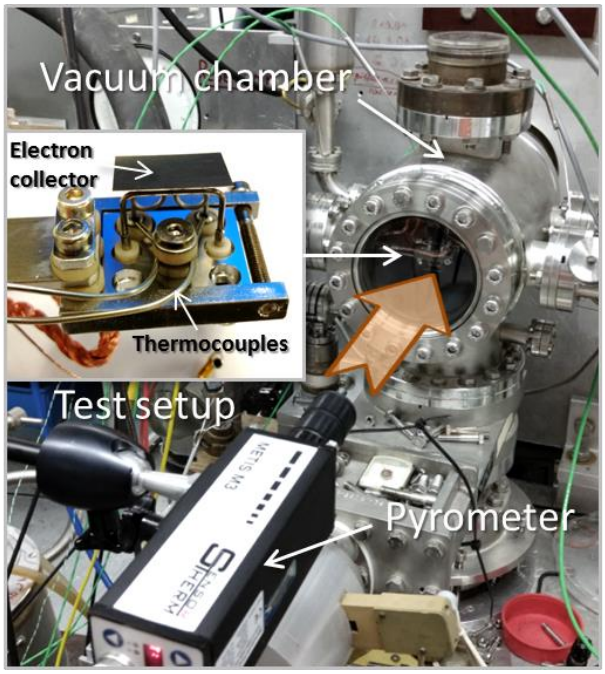

Fig. 2: Experimental setup for measurement of the temperature profile of the filament.

The temperature profile of the filament was measured by means of 1-color radiation pyrometer Metis M313, which performs the temperature measurement in a narrow-band spectral range of 1.27 µm in vacuum and hydrogen atmosphere. This device ideally suits for the measurements of the surface temperature of the components made of tungsten since temperature dependent emissivity characteristics of tungsten cross at the same point corresponding to a wavelength $\lambda = 1.27$ µm and a spectral emissivity $\varepsilon = 0.33$ [4].

The pyrometer is equipped with a color camera module, which provides a composite video output that was connected to a video monitor and via video grabber to a PC. The pyrometer was aligned via a circular reticle on the TV screen. Measuring spot is smaller than 0.6 mm. The camera provides automatic, highly dynamic adjustment of the picture brightness. As the measurement cannot be done continuously along the wire several measurement points have been taken.

The filament temperatures were measured for different heating currents: 15 A, 20 A, 25 A and 30 A. Several minutes to a half an hour is needed to reach thermalized conditions in the filament and the molybdenum supports. The temperature of the supports was measured by means of the thermocouples of type K. Values of the voltage drop along the filament and the electron emission current have been recorded as well. In

all cases potential of electron collector was biased on 250 V in respect with the ground potential.

After the operation of the prototype with heating current of 30 A, the window, through which the measurement was performed, has been partially polluted due to material evaporation under high temperature. In order to correct the effect of this pollution transmission of the window was determined before and after the tests.

Several measurements were done with hydrogen gas at a pressure of 10 Pa. Only the central temperature of the filament has been recorded. Fig. 3 illustrates the effect of gas cooling providing decrease of the temperature on 5 %, which could be considered as negligible.

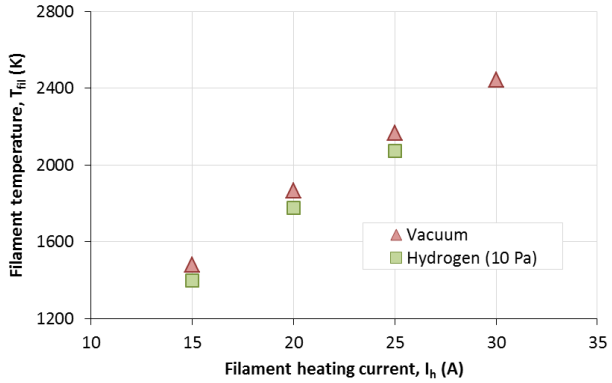

Fig. 3: Filament temperature as a function of heating current for measurements performed in vacuum and with hydrogen pressure of 10 Pa.

3. Thermo-mechanical analysis of the filament

3.1. Description of the model

The model used for the simulations is shown in Fig. 4.

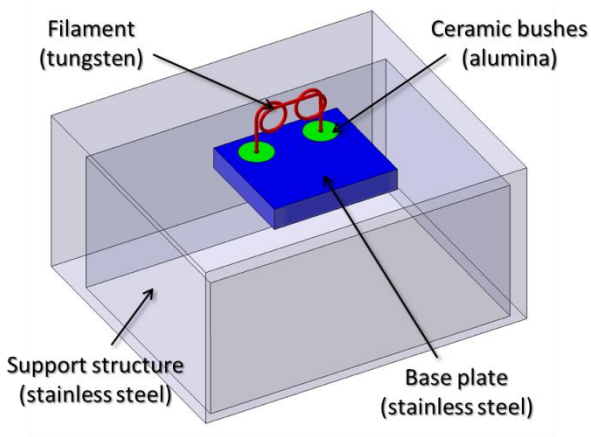

Fig. 4: Simplified model of the DPG head (support structure is transparent).

It should be emphasized that this model was created to simulate a real DPG head, which is noticeably different with respect to the tested prototype (see Fig. 2). In particular, the real gauge has a support structure for accommodation of electrical connections. This component is a part of a simplified model as well. In the real DPG head the filament and all electrodes are covered by means of a metallic cap – the housing with aperture for gas inlet. This cap was not modeled, nevertheless, adjustment of the temperature "seen" by components under the cap was done in order to adapt thermal boundary conditions as close as possible to real conditions. This adjustment is only partially applicable to the simulation of the tested prototype, since instead of the cap, which restricts electrodes and filament from 5 sides, prototype has an electron current collector closes the filament only from above (see Fig. 2).

In the final design of the DPG head the filament will be brazed with the supports, whereas in the prototype the screws are used for the filament fixation in order to have possibility of changing the filament. In this case it is difficult to define exact thermal boundary conditions since it is not possible to say where exactly the filament touches the supports. In the model fixation system is simplified (see Fig. 4). Due to a good thermal and electrical conductivity of a brazing material and low thickness, the contact resistivity is considered negligible. Therefore, a reasonable approach is to consider that the brazing has the properties of one of the brazed materials. The alumina properties are chosen.

3.2. Thermo-electric modelling strategy

The filament is heated by the direct electric current and electrical resistivity produces volumetric heat generation in the filament by the Joule effect. The energy dissipated in the system is the product of the current and the voltage drop. Generated volumetric heat in the filament is fully transferred to the heat sinks under stationary conditions: "conduction" between model elements to a conduction heat sink and "radiation" between model surfaces to a radiation sink. The temperature field resulting from the thermal problem determines the thermal conductivity and also the electrical resistivity of the filament. Thus, electric and thermal problems are solving simultaneously.

3.3. Electrical analysis

The electrical analysis aims at obtaining the Joule volumetric heat generation for the thermal analysis. The voltage at one of the extremes of the filament is set to zero. The current is imposed at the inlet section of the filament. Calculated voltage at the extremes of the filament gives the total voltage drop. The product $\vec{J} \cdot \vec{E}$ of the calculated electric field $\vec{E}$ and the current density $\vec{J}$ determines volumetric Joule heat generation used as an input for the thermal analysis.

3.4. Thermal analysis

The thermal loads are calculated by post-processing of the electrical analysis. Radiation phenomena have been approached in a simplified way, which requires less time for the calculation. It was assumed that each implemented surface (see Fig. 4) interacts with the surrounding environment by means of a single node of given temperature. Since the temperatures of radiation sinks have not been measured directly at the experiment, assumptions were taken respectively (see Table 1).

Table 1: Temperatures seen by the model elements.

Element/Node	"Seen temperature"
Filament	T_AMB_W = 1050 K
Base plate	T_AMB_W = 1050 K
Ceramic bushes	T_AMB_W = 1050 K
Support structure (outer part)	T_AMB = 575 K
Support structure (inner part)	T_AMB_D = 675 K

"Seen" temperature for the filament, the base plate and the ceramic bushes is assumed relatively high since these components are located under electron collector. The support structure does not reflect experimental setup well. Nevertheless, to adapt the model to experimental conditions it was assumed that inner surfaces of this support will see slightly higher temperature than outer part of the support. The effective conduction sink temperature is applied to a bottom part of the support structure. In real conditions DPG head will be welded to the surface of ITER elements – divertor cassette, vacuum vessel or port plug DSM. Modelled prototype was connected to experimental setup in a different way (see Fig. 2). Value of the conduction sink temperature was assumed as T_AMB_D = 675 K. A spatial distribution of the heat generation along the filament is captured by the thermal analysis

3.5. Mechanical analysis

It should be noted that all DPG heads, which will be installed in ITER, have the same design. Even though only 4 of 52 DPG heads will operate at a toroidal magnetic field of 8 T, structural integrity of all gauges shall be confirmed for this environmental condition. Therefore, for calculation of acting $\vec{j}\times\vec{B}$ forces a constant magnetic field of 8 T was applied normally to the filament plane. Thermal stress of the filament was derived from calculated temperature field.

Mechanical elastic analysis resulted in comparison between calculated and "allowable" stresses. The comparison is synthesized by the safety factor value reflecting the ratio between material yield stress at the local temperature and the local Von Mises equivalent stress caused by an acting $\vec{j}\times\vec{B}$ forces and a thermal load. A safety factor greater than one indicates that plasticization does not occur. For cases when safety factor is lower than one, plastic mechanical analysis shall be performed in order to assess a level of the plasticization and a number of cycles that the component can withstand before breaking.

4. Analysis of obtained results and comparison with the experimental data

A temperature distribution in the filament calculated for a heating current of 20 A is shown in Fig. 5.

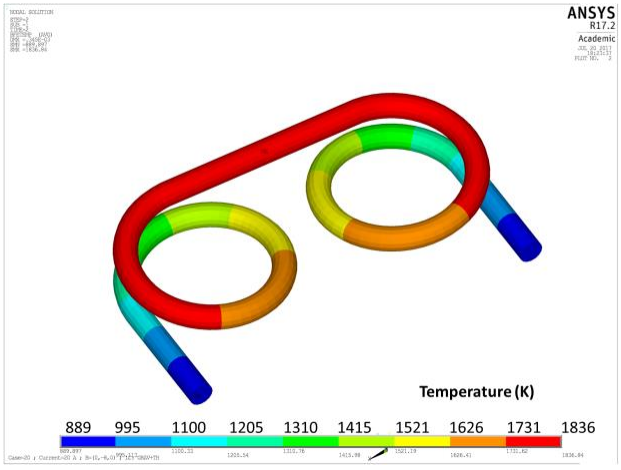

Fig. 5: Temperature distribution in the filament when the filament heating current is 20 A (flipped with respect to Fig. 6).

Photographs in Fig. 6 demonstrate local measurements of the temperature by means of pyrometer when the filament is heated up by a current of 20 A.

Fig. 6: Snapshots from the pyrometer camera taken during temperature measurements of different parts of the filament (heating current is 20 A).

A comparison of calculated filament temperature profile and respective experimental data for several values of the heating current is shown in Fig. 7. The screws fix the filament in the molybdenum supports under the base plate, which makes the effective length of the filament approximately 10 mm longer from each side than in simulations. This is a main reason of substantial difference in the temperatures towards the filament fixation. One can see that for a central part of the filament measured values of the temperature are slightly higher than calculated ones. This may be explained by the fact that base plate in the experiment is insulated from the big structures allowing efficient release of heat by conduction. It should be also noticed that post-test inspection of the prototype showed that the filament fixation screws were untightened. In this case generated heat is also not efficiently released to a conductive heat sink, whereas in simulations a thermal contact was assumed as "ideal".

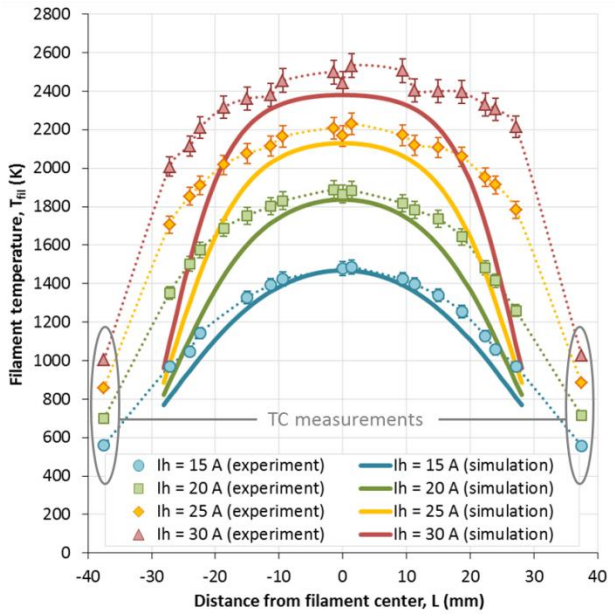

Fig. 7: Comparison of calculated and measured temperature profiles of the filament at different heating currents.

The voltage drop of the filament was measured at the vacuum feedthroughs and then corrected relying on resistivity of the circuit. The voltage drop is strongly dependent on the effective electrical resistivity of the filament. Value of the electrical resistivity in return depends on the temperature and the filament length. Measured values of the temperature are slightly higher than calculated ones (see Fig. 7) and effective length of the tested filament was overall 20 mm longer than in performed simulation. This explains the difference of measured and simulated voltage drops at the filament as shown in Fig. 8. Fig. 8 also reveals that the difference between measured and calculated voltage drop is lower at low heating currents where simulation and experiment match better.

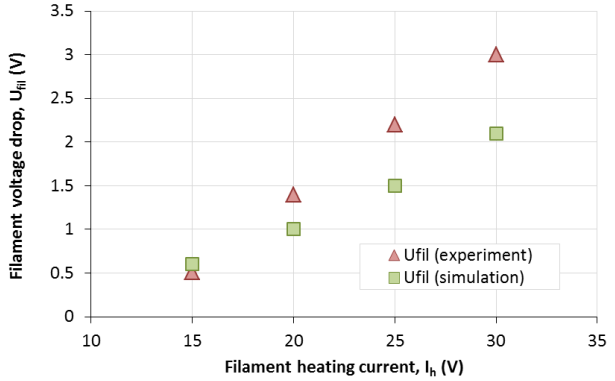

Fig. 8: Comparison of calculated and measured values of voltage drop of the filament at different heating currents.

As mentioned in Section 2 during measurement of the temperature profile electron emission current was recorded. It was found that the heating current of 15 A is not enough to initiate an electron emission from the filament, whereas at the heating current of 20 A emission current appeared. The fact that an electron emission starts when the heating current is between 15 A and 20 A is confirmed by the stand alone test aimed at definition of heating current after 3 month of continuous operation of the prototype in feedback mode when emission current is kept constant (~300 µA) while heating current could vary. At the beginning of the test the heating current was stabilized near a value of 18 A. Although a final conclusion regarding operational value of a heating current shall be taken at the end of the test, at present value of 20 A could be assumed.

Direction of forces acting on the filament heated by a current of 20 A and operated under magnetic field of 8 T (i.e. 160 N/m) is shown in Fig. 9. According to a distribution of Von Mises stresses along the filament (see Fig. 9) the most critical areas in terms of mechanical stability are located near fixation node and at inner part of the spirals. An important result is that for these areas calculated value of safety factor is around 1.4. This means that under considered loads and boundary conditions the filament and, hence, the DPG head will operate without failure due to immediate plastic collapse. This statement, however, shall be confirmed during mechanical rupture and deformation test of the filament.

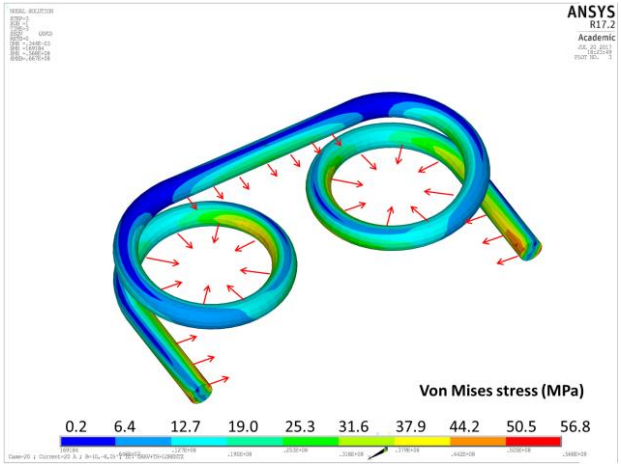

Fig. 9: Direction of acting forces and distribution of Von Mises equivalent stress in the filament heated by a current of 20 A under B-field of 8 T.

5. Conclusions

A simplified parametric model, which allows performing thermo-mechanical assessment of the filament, has been developed. A “single spiral” filament with diameter of 0.8 mm was defined as the optimal one in terms of mechanical stability. For this filament operated with heating current of 20 A and under the magnetic field of 8 T a minimum value of calculated safety factor against the yield stress is 1.4, which indicates a safe operation of the gauge against immediate plastic collapse. This result will be validated during mechanical rupture and deformation test of the filament, which will be performed in autumn 2017.

The temperature profile of the optimized filament was measured by means of 1-color radiation pyrometer for the heating currents of 15 A, 20 A, 25 A and 30 A. Several measurements were done with a hydrogen gas at a pressure of 10 Pa. A comparison between calculated and measured in the experiments temperature profiles of the filament showed a good agreement for the central

part of the filament and deviations towards the filament fixation caused by differences in boundary conditions.

The material properties of the DPG FE model were benchmarked against experimental results.

Acknowledgments

This work was partly supported by Fusion for Energy under the Specific Grant F4E-FPA-364-SG05 and Framework Service Contract F4E-OMF-457-01-10. The views expressed in this publication are the sole responsibility of the authors and do not necessarily reflect the views of the Fusion for Energy and the ITER Organization.

Neither Fusion for Energy nor any person acting on behalf of Fusion for Energy is responsible for the use, which might be made of the information in this publication.

References

[1] G. Haas, H.S. Bosch, Vacuum 51 (1998) 39-46

[2] H. Nielson (Ed.), Magnetic Fusion Energy: From Experiments to Power Plants, Woodhead Publishing Series in Energy: Number 99, Elsevier, (2016), ISBN: 978-0-08-100315-2

[3] A. Arkhipov et al, Journal of Fus. Eng. Des. DOI: 10.1016/j.fusengdes.2016.12.020

[4] De Vos, J.C., Physica, 20, 690, 1954